Experimental Feasibility Assessment of Counter-Rotating Propellers for Stratospheric Airships

Conference Paper · January 2015

DOI: 10.2514/6.2015-1029

4 authors, including:

Zhihao Tang
China Ship Development & Design Center
7 PUBLICATIONS **27** CITATIONS
SEE PROFILE

Hao Guo
Beihang University (BUAA)
67 PUBLICATIONS **330** CITATIONS
SEE PROFILE

AIAA SciTech
5-9 January 2015, Kissimmee, Florida
53rd AIAA Aerospace Sciences Meeting

Experimental Feasibility Assessment of Counter-Rotating Propellers for Stratospheric Airships

Peiqing Liu*, Zhihao Tang†, Yaxi Chen‡, and Hao Guo§
Beihang University, 100191 Beijing, People's Republic of China

A series of systematic wind tunnel tests of a given stratospheric airship counter-rotating propeller have been conducted in this paper. The basic aerodynamic performance of the stratospheric airship counter-rotating propeller has been explored. In addition, different from conventional propellers, the effect of low Reynolds number has been illustrated. Compared with single-rotating propellers, the interference between front and rear propeller has also been discussed. The experimental results indicate that low Reynolds number would strongly reduce the efficiency of counter-rotating propellers. Due to the interference between a pair of propellers, the performance of front propeller gets slightly worse, whereas the performance of rear propeller turns much better. A significant improvement of efficiency of overall CRP would be gained. By comparison with other configuration of propeller propulsion system, it indicates the counter-rotating propeller would be a wise option applied on stratospheric airships.

Nomenclature

A	=	area of cross section of wind tunnel test section, m^2
b	=	chord length of propeller blade element, m
C	=	thickness of propeller blade element, m
C_P	=	propeller power coefficient
C_Q	=	propeller torque coefficient
C_T	=	propeller thrust coefficient
d	=	spacing between front and rear propeller disks, m
D	=	diameter of propeller disk, m
J	=	advance ratio
n	=	rotational speed of propeller (per minute), rpm
n_s	=	rotational speed of propeller (per second), r/s
P	=	power of propeller, W
Q	=	torque of propeller, N m
r	=	radius to propeller blade element, m
R	=	radius to tip of propeller. m
Re	=	Reynolds number
T	=	thrust of propeller, N
V	=	advance velocity of propeller, m/s
χ	=	blade twist angle, deg
η	=	propeller efficiency
μ	=	viscosity coefficient, kg/(m s)
ρ	=	density of air, kg/m^3
κ	=	congestion degree of propeller wind tunnel tests

Subscript

o	=	the real propeller at stratosphere

* Professor, School of Aeronautic Science and Engineering, lpq@buaa.edu.cn.
† Ph.D. Student, School of Aeronautic Science and Engineering, Student Member AIAA.
‡ M.Sc. Student, School of Aeronautic Science and Engineering.
§ Assistant Professor, School of Aeronautic Science and Engineering.

m = the propeller model in wind tunnel tests

I. Introduction

The investigations on stratospheric airships have become a hot issue of the modern aerospace sciences. The great features, such as long-endurance, low-energy-consumption, and high-security, make stratospheric airships extensively used in both military and civilian areas, such as precision navigation, environmental monitoring, communication relays, missile warning, surveillance, and weapon delivery [1-3]. These main advantages of stratospheric airships rely on a propulsion plant with high efficiency. Normally, the open propeller, or airscrew, can offer an efficient means of propulsion for airships that cannot be matched by the high exhaust velocity of a turbojet. Just as turbofan engine is more efficient than a turbojet of the same thrust, a propeller is more efficient than either of them [4]. That is why propeller propulsion system is considered widely utilized on stratospheric airships.

However, the air environment at stratosphere is very different from low altitude (under 10 km), shown as Table 1. When the propeller designed as conventional propeller for low-altitude aircrafts operates at stratosphere, the special flight condition, such as low advance speed and low Reynolds number, makes the propeller performance doomed to be poor [1, 5]. For the lack of appropriate design methods of high-altitude (about 20 km) propellers, Liu [6] has proposed some theoretical concepts of counter-rotating propeller (CRP) propulsion system for stratospheric airships depending on the following prospective benefits:

1) The smaller size can be applied when the CRP provides the same thrust as a single-rotating propeller (SRP).
2) The CRP configuration can balance the torque of two propeller disks.
3) The higher efficiency can be gained than SRP which has the same number of blade in total as CRP.

Table 1. The air environment different from altitude.

Altitude, km	Temperature, K	Air Pressure, Pa	Air Density, kg/m^3	Sound Velocity, m/s	Viscosity, 10^{-5} kg/(m s)
0	288.15	101325	1.2250	340.29	1.7894
10	223.20	2643.6	0.41270	299.46	1.4571
20	216.65	5529.3	0.08891	295.07	1.4216

Many experimental investigations of CRPs have been conducted during last half century, but few of them aimed at application in the circumstance of high altitude and low advance speed. For example, as early as 1940s, a large scale of wind tunnel tests were conducted by Biermann and Gray [7] on CRPs whichever were tractor or pusher configurations. The results indicated an 8% increase than SRPs in efficiencies of CRPs for the tractor position while a 16% increase for the pusher position. After that, greater power absorption and efficiency of dual-rotating propellers than single-rotating ones were found by Biermann and Hartman's wind tunnel test [8] at low advance ratio. Meanwhile, some other research conducted by McHugh and Pepper [9] shown that aerodynamically improved airfoil designs were highly related to the performance of CRPs. Two years later, Gray's [10] experimental study found that the overall efficiency of a CRP was not seriously affected by small changes in blade angle or changes in rotational velocity of the rear propeller. The experiment of effect on the propulsive efficiency of locking or windmilling one propeller of a CRP for both tractor and pusher positions was conducted by Bartlett [11]. It indicated that a CRP with one propeller disabled resulted in a reduction of total propeller efficiency. The experimental study was not with high Mach number until Colehour and Davenport [12] proved in 1985 that an 8% increase in efficiency of CRPs could be gained when Mach number is nearly 0.7. Of course, except the experimental investigations all above, considerable theoretical and computational studies also conducted by many other researchers. All of them exhibited many advantages of CRP system applied on conventional aircraft, such as higher peak efficiency, better off-design performance, and a reduced total torque over SRP system. These improved performance allowed for smaller propulsion units installed on the aircraft.

Nevertheless, in terms of CRPs for stratospheric airships, because of huge difference from the fight conditions of conventional aircraft, it is unknown whether the CRP system perform better than SRP at high altitude. The relevant investigation was so limited until in this paper Liu and his colleague conducted a series of systematic wind tunnel tests of a given stratospheric airship CRP. Furthermore, the different performance of three kinds of configuration of stratospheric airship propulsion system have also been explored.

II. Experimental Setup

A. Testing Facilities

The wind tunnel tests are conducted in Fluid Mechanics Key Laboratory, Ministry of Education of China, which is located in Beihang University. The low-speed low-turbulence closed-circuit aeroacoustic wind tunnel D5 is applied, as shown in Fig. 1. The wind tunnel has a contraction ratio of 9:1. The open test section used in this paper is 2.0 m long with a square cross section of 1.0 m by 1.0 m. The wind speed can be continuously controlled from 0 to 60 m/s by transforming the frequency of the axial-flow compressor. The airflow turbulence intensity is smaller than 0.08%.

Figure 1. The D5 low-speed low-turbulence closed-circuit aeroacoustic wind tunnel.

The main components of the testing and measuring system are shown as Fig. 2. Either of front or rear propeller is connected to a six-component beam strain-gauge balance which is linked to a collector ring at the other end. Each propeller is driven by an electric motor, of which the rated power is 2 kW. The diameter of the electric motor cross section is smaller than 20% of propeller disk diameter. Each of the electric motors is supported by a steel stand and installed on the rotation axis of propeller disk, of which the rotational speed can be continuously controlled from 0 to 1500 rpm by a transducer and measured by a tachometer. The spacing between front and rear propellers in this paper is unchanged, so the steel stands are fixed on an immovable stage. In order to reduce the influence of supporting system in the airflow, the fairing is used and the cross section of steel stands is streamline shaped.

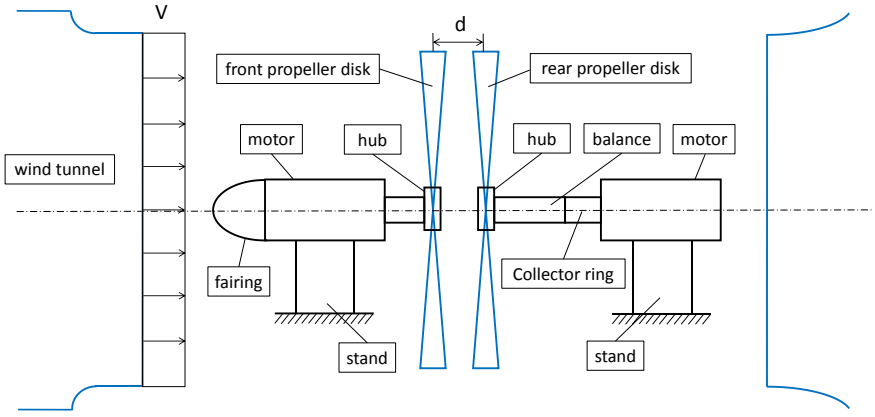

Figure 2. Main components of testing and measuring system.

The installation of testing and measuring system is shown as Fig. 3 and Fig. 4. The thrust and torque of each propeller can be measured by the six-component beam strain-gauge balance. The measurement range and relative error of every component are list in Table 2. The thrust and torque components (X and M_X components in Table 2) of the balance have much wider measurement range than others so that to be hardly interfered by others. The collector ring plays an important role during the measuring process to transmit the electrical signals from the balance with high rotational speed to the data acquisition system. Then, the data acquisition system is responsible for transferring the electrical signals to the force and torque information. The installation of data acquisition system is illustrated in

reference [13, 14]. The balance can be connected to the propeller prepared to test and uninstall the other propeller if the performance of SRP need to be measured.

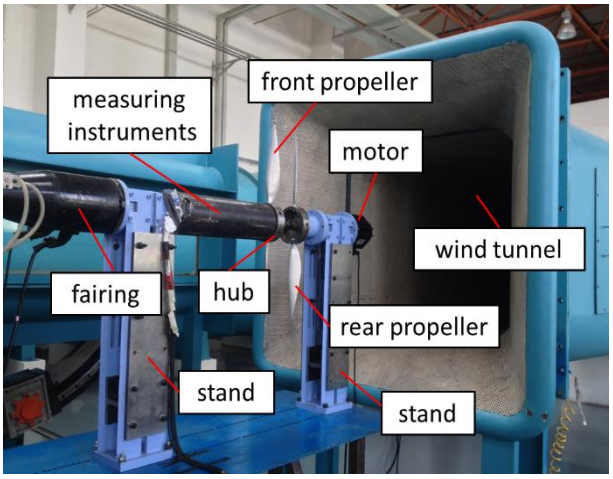

Figure 3. The installation of testing system.

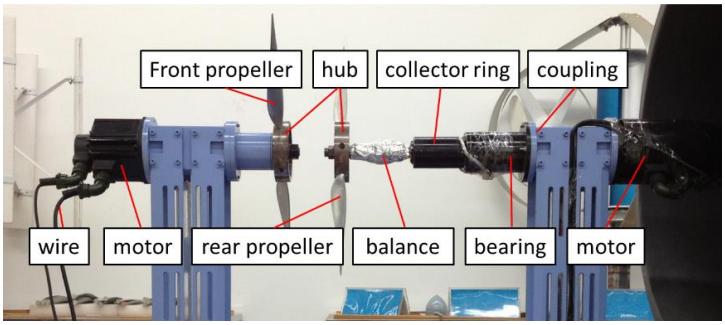

Figure 4. The installation of measuring instruments.

Table 2. Measurement range and relative error of the balance in this experiment.

Component	X	Y	Z	M_X	M_Y	M_Z
Measurement Range, N or N m	300	120	120	60	15	15
Relative Error	0.28%	0.12%	0.39%	0.5%	0.36%	0.12%

B. Experimental Models

With the lack of design method of stratospheric counter-rotating propeller, the CRP model in this experiment is consist of two SRPs. Each of them is optimum designed for a given stratospheric airships independently. The shape parameters of their blades are exactly the same except their converse rotational direction.

The design of CRP model in wind tunnel have to be in accordance with the similarity principle. Generally speaking, it is impossible to keep all similarity parameters equal to real CRP at high altitude. Due to the low advance and rotational speed of stratospheric airship propellers, the Mach number of the real CRP is small enough (usually varying from 0.1 to 0.3), even though the sound speed is much slower at high altitude than near ground. Therefore, the effect of Mach number in this experiment can be neglected and the impact of Reynolds number and advance ratio becomes dominant. It has already been proved by previous investigations that the tests can be conducted in the conventional near-ground wind tunnels when Reynolds number and advance ratio around the model are consistent with the real stratospheric airship CRP [14, 15]. In this paper, the propeller Reynolds number and advance ratio can be defined by equations (1) and (2).

$$\mathrm{Re} = \frac{\rho n_s D^2}{\mu} \tag{1}$$

$$J = \frac{V}{n_s D} \tag{2}$$

Hence the similarity principle applied in this experiment can be summarized by

$$\frac{\rho_o n_{so} D_o^2}{\mu_o} = \frac{\rho_m n_{sm} D_m^2}{\mu_m} \tag{3}$$

$$\frac{V_o}{n_{so} D_o} = \frac{V_m}{n_{sm} D_m} \tag{4}$$

All the parameters of the real CRP at design point have already been determined. As long as the diameter of CRP is confirmed, all the parameters of CRP model can also be determined as well.

The size of model has a close relationship with the size of test section of wind tunnel. When propeller experiment is conducted in wind tunnel, the congestion degree can be defined by

$$\kappa = \frac{\pi R^2}{A} \tag{5}$$

Generally speaking, the congestion degree ought not to beyond 30% in wind tunnels with closed test section, but this rule can be appropriately relaxed when open test section is applied [16, 17]. Hence the size of model seems to be smaller the better. However, it is difficult to full the similarity principle of Reynolds number with so small size of CRP model. In addition, it brings great troubles to manufacture so tiny blade element airfoils and match an appropriate electric motor with tiny size. Therefore, on the other hand, the diameter of propeller model cannot be too small. Finally, considering all the reasons above, the diameter is decided to be 0.75 m. At this moment, the congestion degree remains 44.2%. Then, the performance parameters of CRP model can be calculated by equations (3) and (4) and the shape of the model can be determined on basis of geometric similarity principle, as shown in Table 3 and Fig. 5.

Table 3. The performance parameters.

Parameters	Real Propellers		Experimental Models	
	Front Disk	Rear Disk	Front Disk	Rear Disk
Altitude, km	20		0	
Spacing between Disks, m	0.613		0.115	
Number of Blades	2	2	2	2
Diameter, m	4.0	4.0	0.75	0.75
Rotational Speed, rpm	400	400	1039	1039
Advance Speed, m/s	20	20	9.7	9.7
Pitch Angle, deg	28.3	28.3	28.3	28.3
Airfoil	S1223	S1223	S1223	S1223

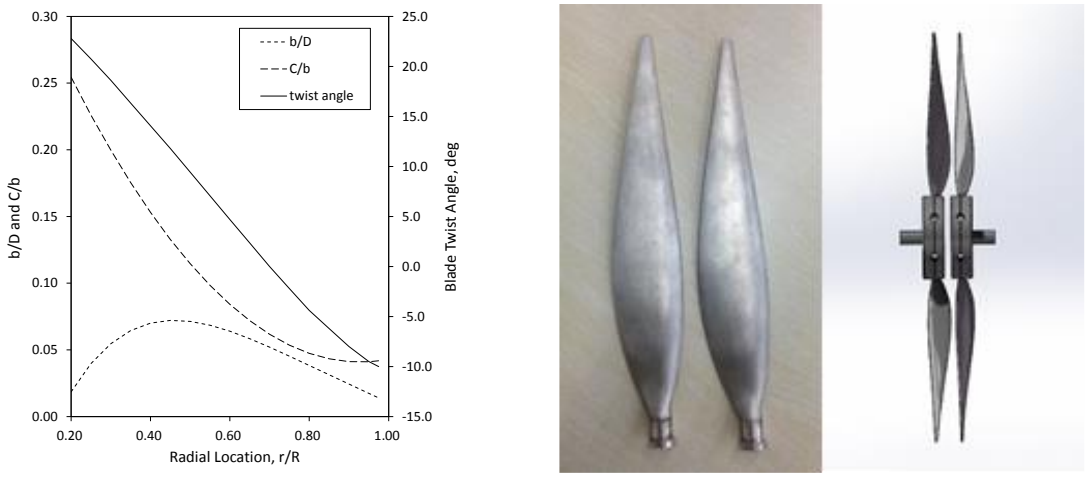

a) **b)**

Figure 5. Shape of the CRP model, a) Chord, thickness, and twist angle, b) Shape of blades.

C. Test Conditions

The wind tunnel tests in this paper can be divided into two parts: one is to explore the basic aerodynamic performance of the given CRP for stratospheric airships and the other is experiment of 2-blade and 4-blade SRPs for comparison (the blade setting is the same as CRP blades). The electric propeller propulsion system with solar power is the latest concept of future high-altitude airship development, of which the rotational speed can be easily changed for varying thrust under different flight conditions [1-3]. Considering the requirement of light weight of airship propulsion system, the CRP is designed with fixed pitch angle. Therefore, the effect of various pitch angle to CRP performance is not a content in the present experiment, even though it is important for future researches. All the test conditions have been list in Table 4. The wind speed and rotational speed in the test conditions have already contained the design point in Table 3.

Table 4. Test conditions.

Test Number	Propeller Type	Number of Blades		Rotational Speed, rpm		Spacing between Two Propellers, m
		Front	Rear	Front	Rear	
1	CRP	2	2	500/750/1000/1250/1500	Equal to Front	0.15
2	SRP	2/4	/	1500	/	/

III. Results and Discussions

All the measured thrust and torque of front and rear propellers of CRP with corrections can be sorted in function of wind speed as Fig. 6 (experiment results of Test 1 in Table 4).

A. Experimental Accuracy

In order to minimize the measurement error, every thrust and torque is requested to be measured 5 times. To evaluate the uncertainty of the testing and measuring system, the Smith Kline method [21] is applied. The uncertainty of the system comes from the measurement error of all the measuring components. The accuracy of every component of the balance is list in Table 2. The rotational speed of propellers is measured by a tachometer within the error of ±5 rpm, while the wind speed by a differential pressure transmitter within 1.0%. Compared with the measurement error of these instruments, the manufacturing accuracy of the model and the installation accuracy of the system is too tiny to consider in uncertainty calculation. The uncertainty under some test conditions has been calculated and list in Table 5. It indicates that the experimental accuracy gets much better at high rotational speed. Therefore, some important characteristics of stratospheric airship CRPs can be discussed at rotational speed of 1500 rpm. When the advance ratio is very large, for example 1.4 in Table 5, the value of thrust coefficient, power coefficient, and efficiency is so tiny that the relative uncertainty is a little large.

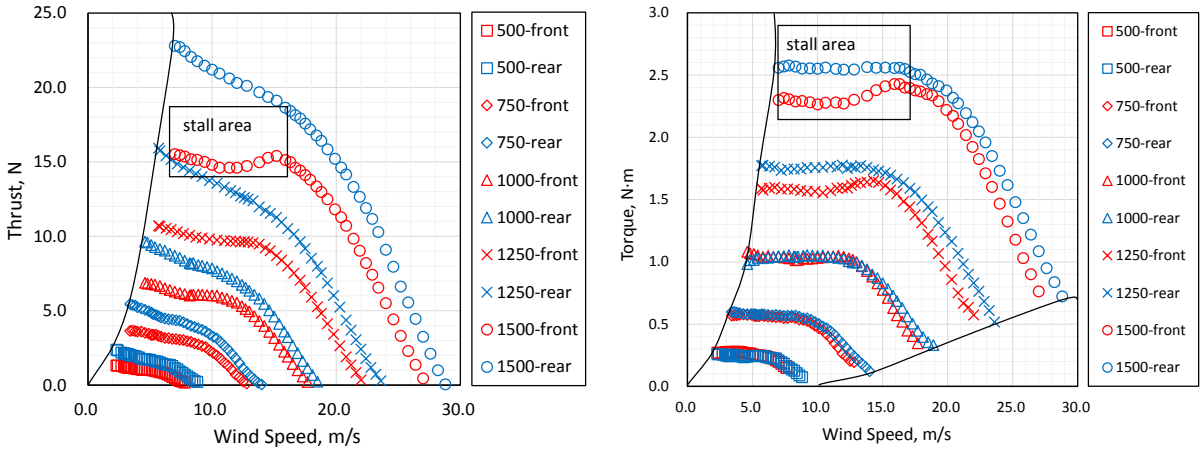

a) b)

Figure 6. Thrust and torque measured of front and rear propeller, a) Thrust, b) Torque.

Table 5. Relative uncertainty under some test conditions.

Rotational Speed, rpm	500		1000			1500		
Advance Ratio	0.6	1.0	0.6	1.0	1.4	0.6	1.0	1.4
Thrust Coefficient, %	3.45	7.85	0.79	0.92	5.29	0.63	0.43	4.88
Power Coefficient, %	3.29	3.96	1.97	2.37	5.96	0.67	0.52	1.21
Efficiency, %	4.85	8.86	2.14	2.57	7.82	0.98	0.64	5.21

B. Effect of Low Reynolds Number

A blade of propeller can be treated as a wing which is consist of a series of blade elements with different angle of attack along the radial location. Every blade element can be regarded as a two-dimension airfoil. The Reynolds number of these airfoils can be determined by

$$\mathrm{Re} = \frac{\rho b \sqrt{V^2 + \left(2\pi n_s r\right)^2}}{\mu} \tag{6}$$

Airfoil S1223 is adopted in this CRP design. The airfoil thickness is different depending on the radial location on the blade. The lift and drag characteristics of S1223 have been investigated in previous research [22-24] and some of the results can be illustrated in Fig. 7. It could be concluded that the lift and drag coefficient of S1223 is different with varying Reynolds number. The differences get greater when the thickness gets bigger. Figure 7d displays the lift-drag ratio of S1223 in function of angle of attack. The ratio shows a great difference at varying Reynolds number. In Glauert's theory [25], the lift-drag ratio of blade element airfoils is closely associate with the efficiency of propeller. Hence it is not difficult to judge that the performance of the stratospheric airship CRP would be affected significantly by varying Reynolds number.

In order to analysis the effect of Reynolds number, some other non-dimension parameters, such as thrust coefficient C_T, power coefficient C_P, and efficiency η, should be introduced here by equations (7) to (9). These parameters can be calculated from measured thrust and torque in Fig. 6, as shown in Fig. 8. The Reynolds number of propellers determined by equation (1).

$$C_T = \frac{T}{\rho n_s^2 D^4} \tag{7}$$

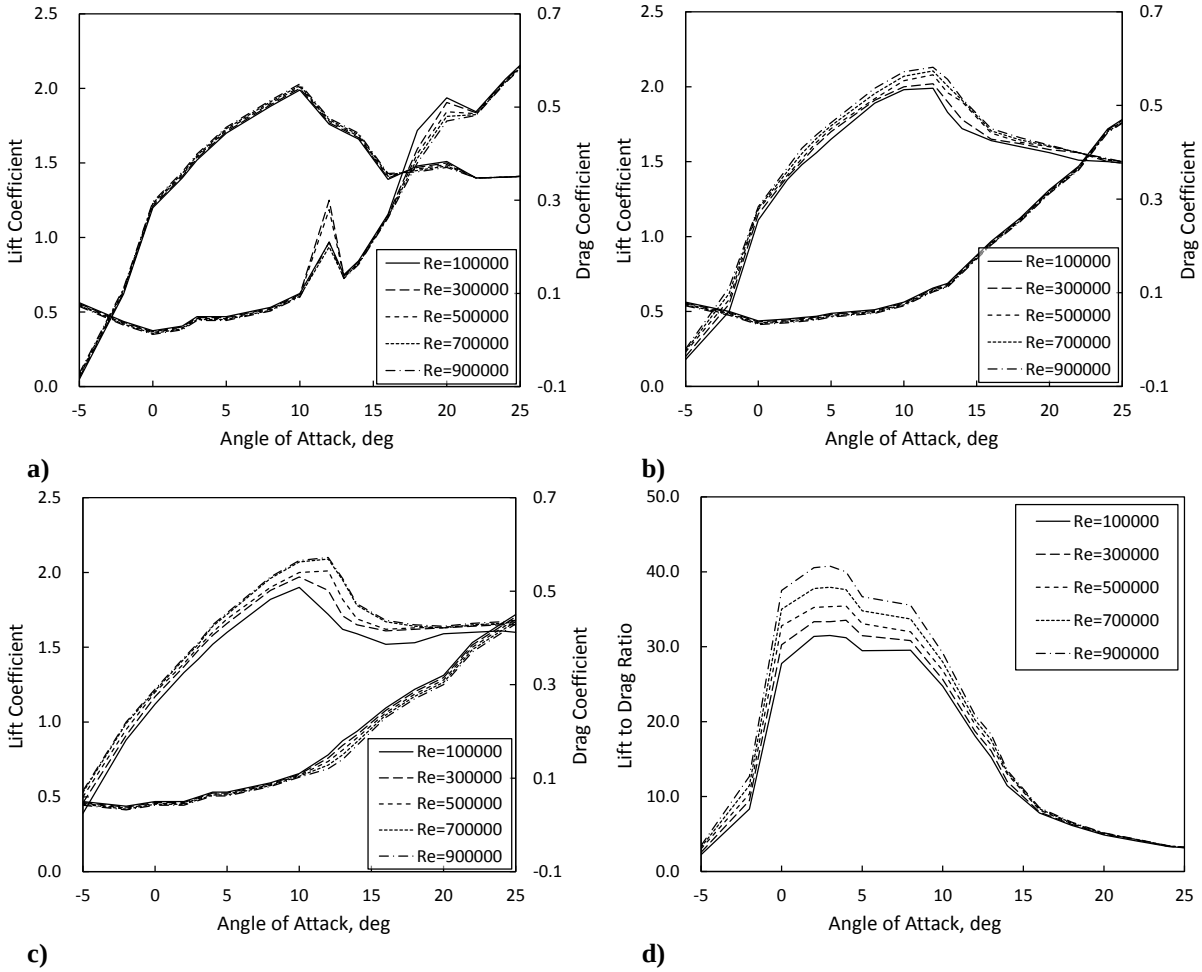

Figure 7. Lift and drag coefficient, or lift-drag ratio of S1223 with different thickness, a) Thickness of 5%, b) Thickness of 12.13%, c) Thickness of 20%, d) Lift-drag ratio with thickness of 12.13%.

$$C_p = \frac{P}{\rho n_s^3 D^5} = \frac{2\pi n_s Q}{\rho n_s^3 D^5} = 2\pi C_Q \tag{8}$$

$$\eta = \frac{TV}{2\pi n_s Q} = \frac{C_T}{C_P} J \tag{9}$$

Normally, Reynolds number around conventional aircraft propeller would reach the order of 10^7. In contrast, that around stratospheric airship CRPs is too low to neglect its influence to the aerodynamic performance. According to Fig. 8, at a certain advance ratio, the thrust coefficient of whatever front or rear propeller, as well as power coefficient and efficiency, is so different with variation of Reynolds number. These non-dimensional parameters achieve additions with the increase of Reynolds number. It indicates the performance of stratospheric airship CRPs and Reynolds number are highly correlated.

Table 6 shows the efficiency of front and rear propeller at some certain advance ratio and varying Reynolds number (rotational speed). Judging from the figures, owing to the worse aerodynamic performance of blade element airfoils with lower Reynolds number, the efficiency of whatever front or rear propeller gets much worse. Whatever the advance ratio is, the effect of Reynolds number is significant until it achieves high enough. However, although the efficiency of propeller gets higher with the addition of Reynolds number, the degree of this improvement becomes smaller. Finally, the efficiency would not be a function of Reynolds number any more. The high efficiency area (higher than 60%) of the given stratospheric airship CRP appears at advance ratio varying from 0.8 to 1.2. The highest efficiency of front propeller is 68% whereas rear propeller is close to 85% when rotational speed is 1500

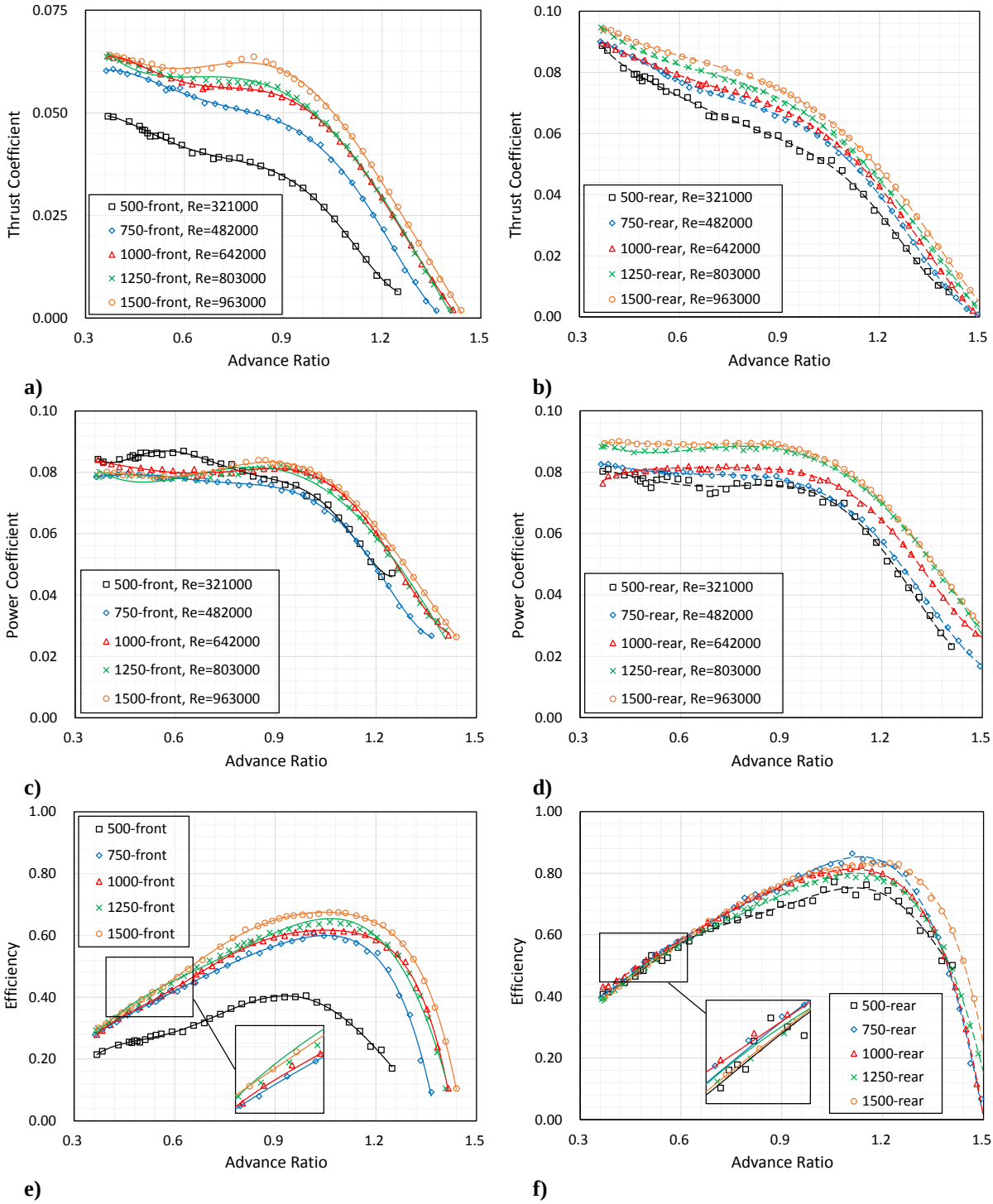

Figure 8. Thrust and power coefficient with varying Reynolds number, a) Thrust coefficient of front propeller, b) Thrust coefficient of rear propeller, c) Power coefficient of front propeller, d) Power coefficient of rear propeller, e) Efficiency of front propeller, f) Efficiency of rear propeller.

rpm. All in all, the low Reynolds number would reduce the CRP efficiency so that the high-altitude CRP design should consider this effect in detail and the experiment should be conducted at the same Reynolds number that it would be flying at.

Table 6. Efficiency of front and rear propeller at varying Reynolds number.

J	0.6		0.8		1.0		1.2	
n, rpm	Front	Rear	Front	Rear	Front	Rear	Front	Rear
500 (Re=3.21×10^5)	29%	56%	38%	67%	41%	71%	24%	73%
750 (Re=4.82×10^5)	42%	58%	52%	72%	61%	81%	54%	83%
1000 (Re=6.42×10^5)	42%	58%	56%	72%	61%	79%	59%	80%
1250 (Re=8.03×10^5)	44%	56%	58%	69%	63%	77%	59%	77%
1500 (Re=9.63×10^5)	47%	59%	62%	72%	66%	81%	64%	83%

C. Interference between Front and Rear Propellers

It could be concluded from Fig. 6 that at a certain rotational speed, the thrust of whatever front or rear propeller decreases with the addition of wind speed. While at a certain wind speed, the thrust of whatever front or rear propeller increases with the addition of rotational speed. On the other hand, because of rear propeller absorbing the swirl energy of front propeller slipstream, the thrust of rear propeller is a little larger than front propeller. Furthermore, the variation regulation of torque is nearly the same, besides it remains almost unchanged at low wind speed. The torque of rear propeller is larger than front propeller as well, although it is not significant. In Fig. 6, the stall area can be found on the thrust and torque curve of front propeller because of airfoil stall at blade elements, while it disappears on rear propeller. It could be proved that absorbing the swirl energy would not only increase the thrust and torque but also improve the performance in stall area.

To analyze the interference between front and rear propeller, taking the test data of 1500 rpm as an example due to the highest accuracy, the thrust coefficient, power coefficient, and efficiency of Test 1 are shown in Fig. 9. The performance of front and rear propeller would exactly like the two-blade SRP if there were no interference between them, but it is definitely not. It would obtain a conclusion from the figures that the interference will affect the performance of each propeller significantly. At the same advance ratio, the performance of front propeller, whatever thrust coefficient, power coefficient, or efficiency, is slightly worse than two-blade SRP, whereas the performance of rear propeller is much better. It means the interference from rear propeller makes the performance of front propeller poorer than it works independently. However, the rear propeller has recovered the energy of swirl airflow in the slipstream of front propeller, which results in that the benefit from the interference due to front propeller is stronger than the loss. In total, due to the much improvement of rear propeller efficiency, the performance of overall CRP is a bit better than the two-blade SRP, especially under the advance ratio over 1.2. The four-blade SRP has the same number of blades as the given CRP overall, but it cannot provide the same thrust and absorb the same power under the same fight conditions. Due to the loss from the interaction among more blades, the efficiency of four-blade SRP is much worse than the given CRP. One else conclusion could be summarized from the figures is the different location of peak efficiency of SRP and CRP. The interference determines not only the value of peak efficiency but also where it appears.

D. Discussions on Different Configuration of Propeller System

After the performance of the stratospheric airship CRP is revealed, the comparison of different configurations of high-altitude airship propulsion system can be discussed. For example, considering a four-blade-propeller system would be applied on a stratospheric airship, there are usually three kinds of configurations: a four-blade SRP, two two-blade SRP, and a pair of CRP with two blades of front and four blades of rear. Which one would be best on the view of aerodynamic performance? It assumes the shape and size of blades are exactly the same as presented above. The efficiency as a function of thrust coefficient or power coefficient is given in Fig. 10.When providing the same thrust, the efficiency of CRP propulsion configuration is the highest, as well as when absorbing the same power. The CRP and the SRP show almost the same efficiency under low thrust coefficient or power coefficient and the superiority of them is not seen. When thrust coefficient or power coefficient gets high, the difference between the CRP and the SRP is significant. This is because one propeller hardly disturbs the other propeller and only a weak swirl velocity to be recovered by rear propeller is generated by the front propeller as the blade loading of each propeller is low. The front propeller leaves enormous swirl velocity behind with the addition of thrust and power, which means a huge loss of energy. This energy is recovered by rear propeller to increase the overall CRP efficiency. However, for the SRP, this energy just flows away. The more blades included, the more energy loses. Therefore, it indicates that CRP system would be a good choice to improve propulsion performance of stratospheric airships.

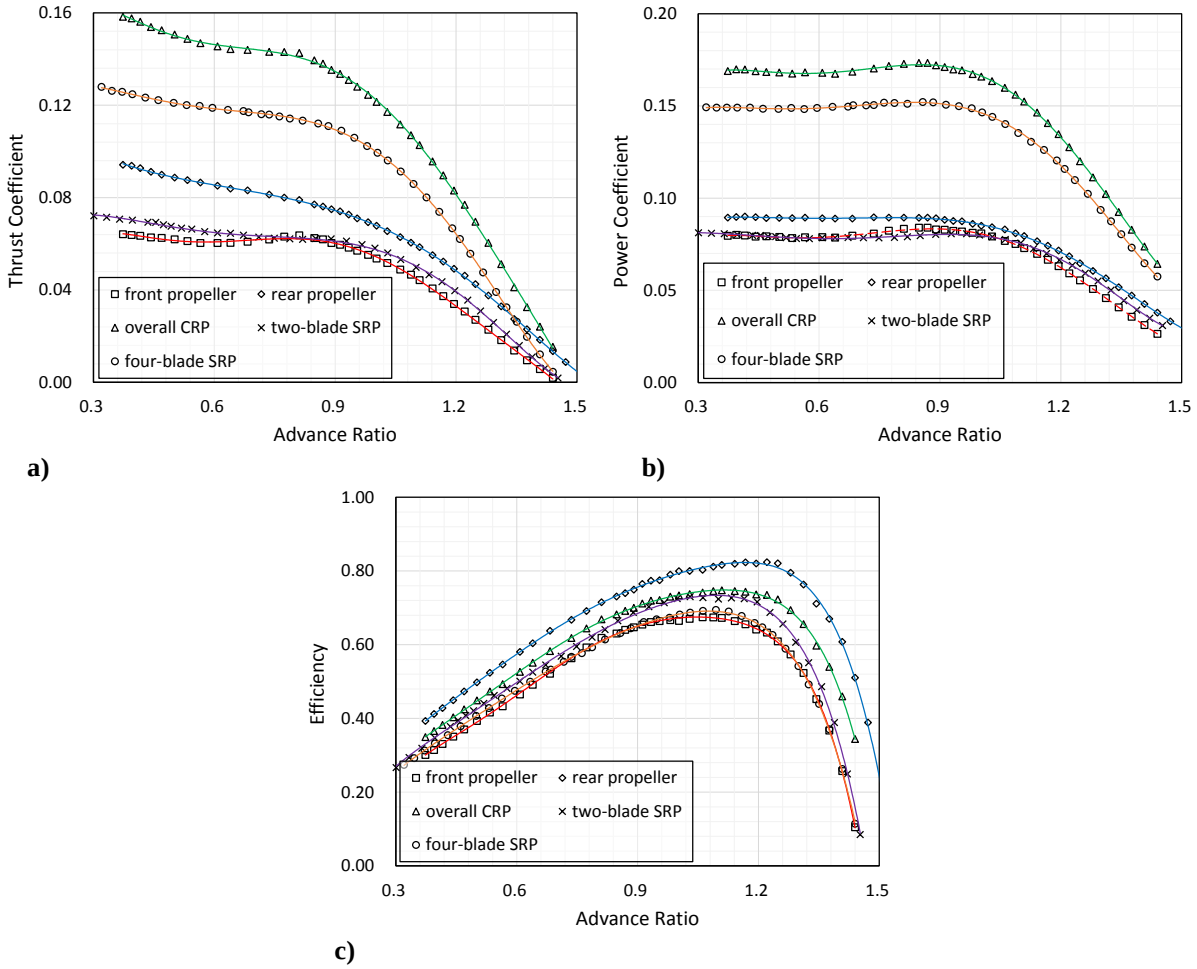

Figure 9. Thrust coefficient, power coefficient, and efficiency of CRP at rotational speed of 1500 rpm with comparison of two- and four-balde SRP, a)Thrust coefficient, b) Power coefficient, c) Efficiency.

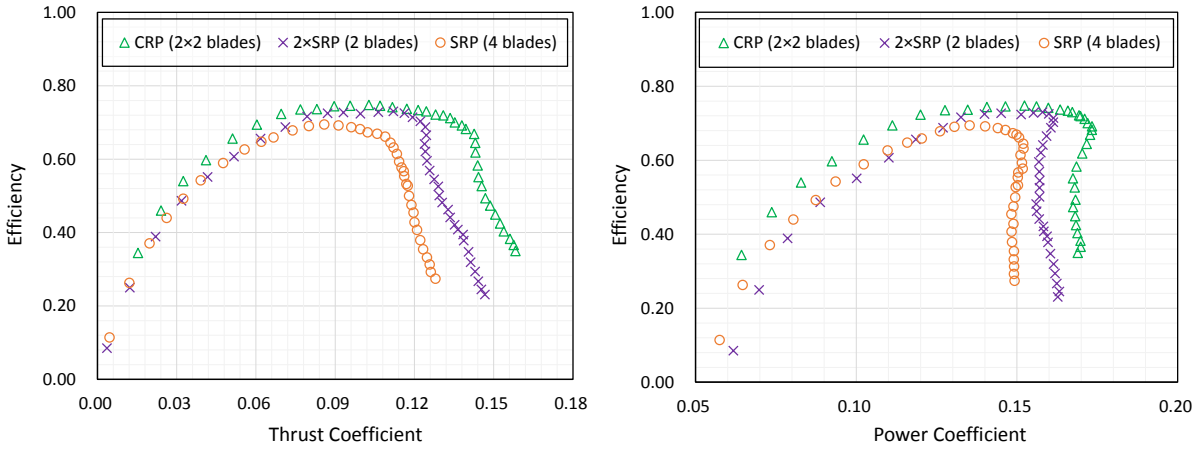

Figure 10. Comparison of different configurations of propeller propulsion system, a) Efficiency related to thrust coefficient, b) Efficiency related to power coefficiency.

IV. Conclusions

A series of systematic wind tunnel tests of a given stratospheric airship counter-rotating propeller have been conducted. According to the experiment, low Reynolds number has a strong effect on the performance of stratospheric airship propellers. This effect would reduce the efficiency so that the high-altitude propeller design should consider the Reynolds number of blade and the experiment should be conducted at the same Reynolds number that it would be flying at. With an optimum design, although the performance of front propeller of CRP gets slightly worse due to the interference from the rear propeller, the performance of rear propeller turns much better as it recovers the energy of swirl airflow in the slipstream of front propeller. A significant improvement of overall CRP efficiency would be gained. Depending on this experiment, the aerodynamic performance of different configurations (two two-blade propellers, one four-blade propeller, or a pair of counter-rotating propellers) is illustrated, which indicates the counter-rotating propeller system would be a wise option applied on stratospheric airships.

However, the investigations on the effect of pitch angle, rotational speed, and number of blades of stratospheric airship CRPs have not been developed yet. It needs to be conducted in the next-step-process in the future.

References

[1]Colozza, A., "Initial Feasibility Assessment of a High Altitude Long Endurance Airship," NASA/CR-2003-212724, Dec. 2003.

[2]Jamison, L., Sommer, G. S., and Porche, I. R., "High-Altitude Airships for the Future Force Army," TR-234-A, Rand Arroyo Center, 2005.

[3]Moomey E. R., "Technical Feasibility of Loitering Lighter-than-Air Near-Space Maneuvering Vehicles," ADA437762, Mar. 2005.

[4]Carichner, G. E., and Nicolai, L. M., *Fundamentals of Aircraft and Airship Design (Volume 2: Airship Design and Case Studies)*, AIAA Education Series, AIAA, New York, 2013, pp. 151-195.

[5]Colozza, A., "High Altitude Propeller Design and Analysis Overview," NASA/CR-1998-208520, Oct. 1998.

[6]Tang, Z., Liu, P., Sun, J., Chen, Y., and Guo, H., "Experimental Investigation of Stratospheric Airship Counter-Rotating Propellers," *Journal of Propulsion and Power* (submitted for publication).

[7]Biermann, D., and Gray, W. H., "Wind-Tunnel Tests of Single- and Dual-Rotating Pusher Propellers Having from Three to Eight Blades," NACA ARR (WR L-359), Feb. 1942.

[8]Biermann, D., and Hartman, E. P., "Wind-Tunnel Tests of Four- and Six-Blade Single- and Dual-Rotating Tractor Propellers," NACA Rept. 747, 1942, pp. 319-347.

[9]McHugh, J. G., and Pepper, E., "The Characteristics of Two Model Six-Blade Counterrotating Pusher Propellers of Conventional and Improved Aerodynamic Design," NACA ARR (WR L-404), Jun. 1942.

[10]Gray, W. H., "Wind Tunnel Test of Dual-Rotating Propellers with Systematic Differences in Number of Blades, Blade Setting and Rotational Speed of Front and Rear Propellers," NACA ARR L4E22 (WR 2-80), May 1944.

[11]Bartlett, W. A., "Wind-Tunnel Tests of a Dual-Rotating Propeller Having One Component Locked or Windmilling," NACA ARR No. L5A13a, Jan. 1945.

[12]Colehour, J. L., and Davenport, F. J., "Analysis of Counter-Rotating Propeller Performance," *AIAA 23rd Aerospace Sciences Meeting*, Reno, Nevada, AIAA-85-0005, Jan. 1985.

[13]Liu, P., Ma, R., Duan Z., and Ma, L., "Ground Wind Tunnel Test Study of the Propeller of Stratospheric Airships," *Journal of Aerospace Power*, Vol. 26, No. 8, Aug. 2011, pp. 1775-1781 (in Chinese).

[14]Ma, R., "Design Technology Study on the High-Efficiency Propeller of the Low Dynamic Vehicles in Stratosphere," Ph.D. Dissertation, School of Aeronautic Science and Engineering, Beihang University, Beijing, 2010 (in Chinese).

[15]Liu, P., Ma, L., Duan, Z., and Ma, R., "Study and Verification on Similarity Theory for Propellers of Stratospheric Airships," *Journal of Beijing University of Aeronautics and Astronautics*, Vol. 38, No. 7, Jul. 2012, pp. 957-961 (in Chinese).

[16]Liu, P. Q., *Theory and Application of Airscrews*, Beihang University Press, Beijing, June 2006 (in Chinese).

[17]Khoury, G. A., *Airship Technology (Second Edition)*, Cambridge University Press, Cambridge, England, UK, 2012.

[18]Glauert, H., "Wind Tunnel Interference on Wing, Bodies, and Airscrews," ADA953012, Sep. 1933.

[19]Pope, A., and Rea, W. H., *Low-Speed Wind Tunnel Testing (Second Edition)*, New York Wiley, 1984.

[20]Oliveira, L. F. Q., and Ceron-Munoz, H. D., "Aerodynamic Analysis of High Rotation and Low Reynolds Number Propeller," *48th AIAA/ASME/SAE/ASEE Joint Propulsion Conference and Exhibit*, Atlanta, Georgia, AIAA 2012-3838, Jul.-Aug. 2012.

[21]Kline, S. J., "The Purpose of Uncertainty Analysis," *Journal of Fluids Engineering*, Vol. 107, Jun. 1985, pp. 153-160.

[22]Ma, R., and Liu, P., "Numerical Simulation of Low-Reynolds-Number and High-Lift Airfoil S1223," *Proceedings of the World Congress on Engineering*, Vol. 2, London, UK, July 2009.

[23]Selig, M. S., and Guglielmo, J. J., "High-Lift Low Reynolds Number Airfoil Design," *Journal of Aircraft*, Vol. 34, No. 1, Jan.-Feb. 1997, pp. 72-79.

[24]Shyy, W., Klevebring, F., Nilsson, M., Sloan, J., Carroll, B., and Fuentes, C., "Rigid and Flexible Low Reynolds Number Airfoils," *Journal of Aircraft*, Vol. 36, No. 3, May-June 1999, pp. 523-529.

[25]Glauert, H., *The Elements of Aerofoil and Airscrew Theory*, Cambridge University Press, Cambridge, England, UK, 1983.

[26] Wald, Q. R., "The Aerodynamics of Propellers," *Progress in Aerospace Sciences*, Vol. 42, No. 2, 2006, pp. 85-128.

[27]Gamble, D. E., and Arena, A., "Automated Dynamic Propeller Testing at Low Reynolds Numbers," *48th AIAA Aerospace Sciences Meeting Including the New Horizons Forum and Aerospace Exposition*, Orlando, Florida, AIAA 2010-853, Jan. 2010.